I.O.S.

THE APPLICATION OF NUMERICAL MODELS TO STORM SURGE PREDICTION

by

R A FLATHER AND A M DAVIES

REPORT NO 16

1975

NATURAL ENVIRONMENT RESEARCH COUNCIL

INSTITUTE OF OCEANOGRAPHIC SCIENCES

INSTITUTE OF OCEANOGRAPHIC SCIENCES

THE APPLICATION OF NUMERICAL MODELS TO STORM SURGE PREDICTION

by

R A FLATHER AND A M DAVIES

REPORT NO 16

1975

Institute of Oceanographic Sciences
Bidston Observatory
Birkenhead
Cheshire L43 7RA

ABSTRACT

The initial stages of an investigation aimed at setting up a new system for the prediction of storm surges in the North Sea are described. The proposed scheme is based on the use of dynamical finite-difference models of the atmosphere and of the sea, the atmospheric model providing the necessary forecasts of meteorological data. This data is converted into the form required for input to the sea model, which then computes the associated storm surge.

Some preliminary results are presented and discussed and an indication given of the further development of the system.

CONTENTS Page

1. INTRODUCTION

During recent years, the use of primitive equation models for simulating atmospheric motion has become well-established. Further, many of the problems associated with the application of these methods to the forecasting situation have been overcome, with the result that numerical models are now being employed in routine weather prediction.

Finite-difference techniques, employed in the above work, have also been widely used to solve the differential equations governing the motion of the sea under the action of tidal and meteorological forces, demonstrating the potentialities of sea models for storm surge prediction (Heaps 1969; Duun-Christensen 1971). However, in previous surge computations, the necessary meteorological data has been either obtained from observations and therefore available only for hindcasts, or extracted by hand from weather charts - a cumbersome and to some extent subjective procedure, not well suited to operational forecasting. Further, the data derived has often taken the form of representative averages over a small number of quite large areas of the sea. In the present paper a description is given of a preliminary scheme, which seeks to overcome these difficulties by linking a numerical model of the atmosphere to one of the sea in a single dynamical surge prediction system. The essence of the proposed scheme is first to obtain forecast meteorological fields from the atmospheric model and then to process the data to give wind stress components and gradients of atmospheric pressure at individual grid points of the sea model, finally using this model - with the processed data as input - to predict the associated storm surge. The main advantage of the approach is that the procedures involved may be readily carried out by computer, since data exists throughout in digital form on regular meshes.

The long-term objective in applying the method to the North Sea is to establish an operational system for water level forecasting based on dynamical techniques. The requirements of such a system are to give warning of possible flooding of low lying coastal areas around the Southern Bight; to provide, in advance, information needed for the successful operation of the future Thames Barrier; and to predict water levels offshore so as to facilitate safe navigation by deep draught vessels in the shallow

approaches to ports in the region. Although tidal variations are not as yet taken into account, the scheme in its present form is capable of producing a genuine forecast of meteorologically generated disturbances. The forecast could be available up to 18 hours before the start of the 12-hour period to which it applies. Much work, however, remains to be done to improve the results, whose accuracy depends on the success of each stage in the prediction procedure.

A two-dimensional finite difference model developed from that described by Heaps (1969) is used for the sea. The Bushby-Timpson ten-level model on a fine mesh (Benwell, Gadd, Keers, Timpson and White 1971) currently employed in weather forecasting at the U.K. Meteorological Office, Bracknell, provides the atmospheric data. This data takes the form of hourly values of the height, H , of the 1000 mb pressure surface at points of the meteorological model grid, a section of which is shown in Figure 1 together with the spatial mesh of the sea model covering the continental shelf surrounding the British Isles. Assuming the hydrostatic law, the heights are converted into atmospheric pressures, so that by taking appropriate differences, east and north components of pressure gradient and subsequently of the geostrophic wind can be deduced. An empirical relation then gives the surface wind in terms of the geostrophic wind and, with a suitable drag coefficient, a quadratic law is used to calculate wind stresses. Finally the meteorological grid point values of east and north gradients of atmospheric pressure and east and north components of wind stress, derived using the above procedure, are interpolated to each point of the sea mesh where they constitute the input data required for the surge calculation using the sea model.

A number of test computations have been carried out covering two surge periods : one of four days, 26 - 30 March 1972; and another of ten days, 28 March - 6 April 1973. The forecasts were evaluated by comparing calculated surge heights with residuals - values of (observed water level - predicted tide) - at several coastal stations around the North Sea. Some of the results are presented in Section 4. In particular, solutions obtained when different conditions are applied on the open boundary of the sea model are examined. The aim here has been to choose a suitable condition which permits incoming surges to be specified on the

boundary, while preventing reflection from the boundary of outward propagating disturbances generated within the model. Further, an attempt is made to assess the importance of tidal friction by comparing solutions of the basic non-linear equations for the sea in which no account is taken of the tides, and a linearised version in which a background level of frictional dissipation due to tides is assumed.

2. THE SEA MODEL

(a) Equations of motion and continuity.

The dynamical equations for storm surges have been used in a number of different forms incorporating various assumptions (Proudman 1954; Reid and Bodine 1968; Duun-Christensen 1971). Following Duun-Christensen but taking east-longitude and latitude as space co-ordinates, the depth-averaged equations are

$$\frac{1}{R\cos\varphi}\left\{\frac{\partial}{\partial\chi}(Du)+\frac{\partial}{\partial\varphi}(Dv\cos\varphi)\right\}+\frac{\partial\zeta}{\partial t}=0\,, \tag{1}$$

$$\frac{\partial u}{\partial t}-2\omega\sin\varphi\, v=-\frac{g}{R\cos\varphi}\frac{\partial\zeta}{\partial\chi}-\frac{1}{\rho R\cos\varphi}\frac{\partial p_a}{\partial\chi}+\frac{1}{\rho D}\left(F^{(S)}-F^{(B)}\right), \tag{2}$$

$$\frac{\partial v}{\partial t}+2\omega\sin\varphi\, u=-\frac{g}{R}\frac{\partial\zeta}{\partial\varphi}-\frac{1}{\rho R}\frac{\partial p_a}{\partial\varphi}+\frac{1}{\rho D}\left(G^{(S)}-G^{(B)}\right), \tag{3}$$

where the notation is :

χ , φ	east-longitude and latitude, respectively
t	time
ζ	elevation of the sea surface
u , v	components of the depth mean current
$F^{(S)}$, $G^{(S)}$	components of wind stress on the sea surface
$F^{(B)}$, $G^{(B)}$	components of the bottom friction
p_a	atmospheric pressure on the sea
D	total depth of the water $= h+\zeta$
h	undisturbed depth of the water
ρ	density of the water, assumed uniform

R mean radius of the Earth

g acceleration of the Earth's gravity

ω angular speed of rotation of the Earth

The component directions are those of increasing χ, φ respectively, i.e. to the east and to the north. The depth-mean currents are defined as

$$U = \frac{1}{D}\int_{-h}^{\zeta} u'\,dz \,, \qquad V = \frac{1}{D}\int_{-h}^{\zeta} v'\,dz \,, \tag{4}$$

where u', v' are components of horizontal current at depth z below the sea surface. Advective terms, which are generally small in the sea (Brettschneider 1967), are omitted in Equations (2) and (3).

A quadratic law relating bottom stress to the depth mean current may be adopted, giving

$$F^{(B)} = k_b \rho U (U^2+V^2)^{1/2} \,, \quad G^{(B)} = k_b \rho V (U^2+V^2)^{1/2} \,, \tag{5}$$

where k_b is a constant for which an appropriate value is 0.0025 (Proudman 1953). The system (1) to (3) with (5) is non-linear. Alternatively, on the basis of work by Bowden (1953,1956) it may be assumed that

$$F^{(B)} = k\rho U \,, \quad G^{(B)} = k\rho V \,, \tag{6}$$

with $k = 0.0024$ ms^{-1}, the value estimated by Weenink (1958) for the southern North Sea. Further, if $\zeta \ll h$, which is generally true in water of sufficient depth, then D may be replaced by h and the system (1) to (3) with (6) is linear.

The problem is then to solve Equations (1) to (3) to find the variations of ζ, U, V over the sea area, given the changing distributions of wind stress and atmospheric pressure at the sea surface.

(b) Initial and boundary conditions

Because of the high rate of frictional dissipation in shallow seas, disturbances are damped quite rapidly, so that after one or two days the influence of the initial conditions becomes negligible

in comparison with effects produced by the meteorological forcing functions. It is usual in hindcasting to take advantage of this fact by assuming that surges are generated from an initial state of rest,

$$\zeta = u = v = 0 \quad \text{at} \quad t = 0, \tag{7}$$

starting the calculation one or two days before the beginning of the period of real interest. When a long-term computation is under way, it may be divided conveniently into shorter sections by taking as initial conditions for any one leg the final values of elevation and current from the preceding leg. Thus, once an operational system has been established, initial conditions will always be available in the form of fields calculated and stored during the preceding forecast. Special initialization techniques, such as those for obtaining balanced fields for the atmosphere (Temperton 1973) and for incorporating observational information (Williamson and Kasahara 1971), have not yet been applied to the sea, though their use may prove to be beneficial in a practical prediction scheme.

Conditions on ζ, u, v must also be satisfied along the lateral boundaries of the sea region. Thus, along a coastline, the normal component of current vanishes giving

$$q_n = 0 \quad \text{for all} \quad t \geq 0 \tag{8}$$

where $q_n = u \sin\beta + v \cos\beta$ and β denotes the direction of the outward normal to the coast measured clockwise from North. Several alternative conditions exist for open sea boundaries. First, elevation may be specified as a function of position and time

$$\zeta = \hat{\zeta}(x, y, t) \tag{9}$$

where $\hat{\zeta}$ represents the disturbance propagating across the boundary. A particular case of condition (9) for surges has $\hat{\zeta}(x, y, t) \equiv 0$ (Veltkamp 1954, Groen and Groves 1962, Heaps 1969). However, as pointed out by Reid and Bodine (1968), such conditions do not take proper account of the damping due to the transfer of energy from the model to the neighbouring sea. Reid and Bodine suggested that a radiation condition would be

more appropriate. Suppose $\hat{\zeta}$ is the elevation associated with the externally generated surge entering the model. Then, since ζ is the total elevation, the internally generated disturbance reaching the boundary is $\zeta' = \zeta - \hat{\zeta}$. Applying a radiation condition to this part of the surge to ensure that its energy propagates outwards gives

$$hq_n' = A'\zeta', \tag{10}$$

where q_n' is the associated outward going current across the boundary and A' is an appropriate admittance coefficient (with dimensions of velocity). To close the problem, the current $\hat{q}_n$ accompanying the input disturbance $\hat{\zeta}$ must be specified. If it is assumed that $\hat{q}_n = 0$, then since $q_n = \hat{q}_n + q_n'$, the condition which results is

$$hq_n = A'(\zeta - \hat{\zeta}). \tag{11}$$

Here $\hat{\zeta}(x, y, t)$ is to be prescribed so that (11) simply relates the normal component of current to elevation at the boundary. Alternatively, since surge energy enters the model, it might be argued that a radiation condition should also be applied to this incoming part of the motion, giving

$$h\hat{q}_n = -\hat{A}\hat{\zeta}, \tag{12}$$

where $\hat{A}$ is an admittance coefficient and the negative sign indicates that the energy transfer is inward. Then from Equations (10) and (12)

$$hq_n = A'(\zeta - \hat{\zeta}) - \hat{A}\hat{\zeta}. \tag{13}$$

In the present work, the admittance coefficients have been taken to be the local free wave speed, so that

$$A' = \hat{A} = (gh)^{1/2}. \tag{14}$$

It should be pointed out that in order to use (9), (11) or (13) in a surge prediction scheme, forecast values of $\hat{\zeta}(x, y, t)$ must be provided. In the present system these are estimated from the meteorological forecast data as described in Section 3.

(c) The finite difference procedure

Equations (1) to (3) are now represented by finite-difference approximations. Introduce the following definitions of finite difference operators :

$$\delta_x(F_t) = \{ F(x+\tfrac{1}{2}\Delta x, \varphi, t) - F(x-\tfrac{1}{2}\Delta x, \varphi, t)\} / R\cos\varphi\,\Delta x$$

$$\delta_\varphi(F_t) = \{ F(x, \varphi+\tfrac{1}{2}\Delta\varphi, t) - F(x, \varphi-\tfrac{1}{2}\Delta\varphi, t)\} / R\,\Delta\varphi$$

$$\overline{F_t}^{x} = \tfrac{1}{2}\{ F(x+\tfrac{1}{2}\Delta x, \varphi, t) + F(x-\tfrac{1}{2}\Delta x, \varphi, t)\}$$

$$\overline{F_t}^{\varphi} = \tfrac{1}{2}\{ F(x, \varphi+\tfrac{1}{2}\Delta\varphi, t) + F(x, \varphi-\tfrac{1}{2}\Delta\varphi, t)\}$$

and $\tilde{F}_t = \overline{\overline{F_t}^{x}}^{\varphi} = \overline{\overline{F_t}^{\varphi}}^{x}$

$$= \tfrac{1}{4}\{ F(x+\tfrac{1}{2}\Delta x, \varphi+\tfrac{1}{2}\Delta\varphi, t) + F(x+\tfrac{1}{2}\Delta x, \varphi-\tfrac{1}{2}\Delta\varphi, t) + F(x-\tfrac{1}{2}\Delta x, \varphi-\tfrac{1}{2}\Delta\varphi, t) + F(x-\tfrac{1}{2}\Delta x, \varphi+\tfrac{1}{2}\Delta\varphi, t)\}$$

where Δx, $\Delta\varphi$ are grid increments in the x and φ -directions, respectively. Then the non-linear system (1) to (3) with (5) is replaced by

$$\zeta_{t+\tau} = \zeta_t - \tau\{ \delta_x(\overline{D_t}^{x} u_t) + \delta_\varphi(\overline{D_t}^{\varphi} v_t \cos\varphi)/\cos\varphi \} \qquad (15)$$

$$u_{t+\tau}\{ 1 + k_b\tau(u_t^2+\tilde{v}_t^2)^{1/2}/\overline{D_t}^{x} \}$$

$$= u_t + 2\omega\tau\sin\varphi\,\tilde{v}_t - g\tau\delta_x(\zeta_{t+\tau}) - \tau\rho^{-1}(P + F^{(s)}/\overline{D_t}^{x}) \qquad (16)$$

$$v_{t+\tau}\{ 1 + k_b\tau(\tilde{u}_t^2+v_t^2)^{1/2}/\overline{D_t}^{\varphi} \}$$

$$= v_t - 2\omega\tau\sin\varphi\,\tilde{u}_{t+\tau} - g\tau\delta_\varphi(\zeta_{t+\tau}) - \tau\rho^{-1}(Q + G^{(s)}/\overline{D_t}^{\varphi}) \qquad (17)$$

where subscripts attached to dependent variables ζ, u, v and D ($= h+\zeta$) refer to time levels, τ is the timestep, $P = \frac{1}{R\cos\varphi}\frac{\partial p_s}{\partial x}$ and $Q = \frac{1}{R}\frac{\partial p_s}{\partial\varphi}$. When taken in the order indicated, Equations (15), (16) and (17) may be solved explicitly for $\zeta_{t+\tau}$, $u_{t+\tau}$, $v_{t+\tau}$, respectively, thereby advancing the solution by one timestep. Repeated solution of the equations allows the motion to be built up through time in the usual way.

The incorporation of some averaging in the system permits

the use of a staggered spatial grid (Platzman 1958, Leendertse 1967) as shown in Figure 2, where ζ is defined at 'O' points, u at '+' points, and v at 'x' points. Depth, h, is defined at the same points as elevation, while P and $F^{(s)}$ are specified at u-points; Q and $G^{(s)}$ at v-points. All boundaries within the model are represented as closely as possible by line segments consisting of sides of the grid boxes. Figure 2 shows an example, in which the open sea boundary is a pecked line and the coastal boundary is shaded. With this restriction on the permitted location and direction of model boundaries, the coastal condition (8) reduces to

$$u_t = 0 \quad \text{for all} \quad t \geq 0$$

at a point on a north-south segment of coast, and

$$v_t = 0 \quad \text{for all} \quad t \geq 0$$

at a point on an east-west segment. The application of open boundary conditions is less straightforward. When elevation is to be specified, as in (9), then following Heaps (1972), $\zeta_{t+\tau} = \hat{\zeta}(x, y, t+\tau)$ and $\zeta_t = \hat{\zeta}(x, y, t)$ are prescribed at elevation points adjacent to the boundary, so that the continuity equation (15) can be rearranged to give the current across the boundary at time t in terms of known quantities. At convex corners on the open boundary, one further relation is needed since two components of current are to be determined. Here, extrapolation from internal values of currents is used to close the problem. Conditions (11) and (13) are somewhat less difficult to apply. First $\zeta_{t+\tau}$ for boundary boxes is calculated from (15) as in the interior of the model. Then using the prescribed value of $\hat{\zeta}$ at this time, the current across the open boundary, $u_{t+\tau}$ or $v_{t+\tau}$, is obtained easily from (11) or (13). In this case, the order of computation starting from ζ_t, u_t, v_t is

(i) calculate $\zeta_{t+\tau}$ from continuity (15);

(ii) calculate currents across the open boundary, $u_{t+\tau}$ or $v_{t+\tau}$ from (11) or (13) using prescribed values of elevation;

(iii) calculate $u_{t+\tau}$ at all internal points from (16), using prescribed values of P and $F^{(s)}$;

(iv) calculate $v_{t+\tau}$ at all internal points from (17), using prescribed values of Q and $G^{(s)}$;

giving $\zeta_{t+\tau}$, $u_{t+\tau}$, $v_{t+\tau}$. A slightly modified procedure is required when (9) is used.

An analysis of the stability of a linearised version of the scheme in Cartesian co-ordinates has been carried out by Flather (1972), who found that a sufficient condition was

$$\tau < \{(1 - \tfrac{1}{2}|f|\tau)/2gh\}^{1/2}\Delta s \qquad (18)$$

where $f = 2\omega\sin\varphi$, the Coriolis parameter, and Δs is the grid space. The implied restriction $\tau < 2/|f|$ is not of practical consequence since the minimum value of $2/|f|$ is about 4 hours, occurring at the poles. Therefore (18) approximates closely the standard Courant-Friedrichs-Lewy criterion.

In applying the scheme to the North Sea, the representation of boundaries and the depth distribution were taken directly from Model 2 of Heaps (1969). The mesh appears in Figure 1 with individual grid points suppressed. The numerical values of constants as yet undefined were taken as follows :

$$R = 6.37 \times 10^6 \text{ m}, \quad g = 9.81 \text{ ms}^{-2}, \quad \rho = 1025 \text{ kg m}^{-3}$$

$$\omega = 7.292 \times 10^{-5} \text{ rad s}^{-1}, \quad \Delta\lambda = 30' \quad \Delta\varphi = 20'. \quad \tau = 180\text{s}.$$

With this choice of constants, the minimum grid spacing is about 26 km so that, according to (18), the maximum permissible depth is 2200 m. Since this value is nowhere reached within the model, the requirements of stability are met.

The computer program written to perform the sea model calculations was designed to read fields of $P, Q, F^{(s)}, G^{(s)}$ and $\hat{\zeta}$ at intervals from data sets stored on magnetic disc. Provided these fields contain forecast values, the solution obtained is a prediction of the surge.

3. THE METEOROLOGICAL DATA

(a) The forecast data

At the Meteorological Office, ten-level model forecast runs of duration 36 hours are carried out twice a day. For the purpose of the present investigation, hourly values of the geopotential height, H, of the 1000 mb pressure surface at grid points covering the north-west European continental shelf (Fig. 1), were stored on magnetic tape. Hours 6 to 18 of each forecast were selected, giving a set of 13 spatial arrays of data spanning the 12 hour period covered. All forecast quantities

required for input to the sea model have to be derived from the geopotential heights. The derivation involves the use of similar assumptions and empirical relationships to those introduced in earlier surge calculations (Heaps 1969, Duun-Christensen 1971). We consider first the treatment of each spatial array of values, and then application of the processed data to the sea model through time.

(b) Treatment of the data

The Cartesian system (x, y), used as horizontal co-ordinates in the atmospheric model, is defined in terms of latitude and east-longitude using the stereographic map projection as follows :

$$x = \frac{2R}{a} \tan\left(\frac{\pi}{4} - \frac{\varphi}{2}\right) \sin(\chi + 35^{\circ}),$$
$$y = -\frac{2R}{a} \tan\left(\frac{\pi}{4} - \frac{\varphi}{2}\right) \cos(\chi + 35^{\circ}), \qquad (19)$$

where a is the grid length at the pole, so that x, y are dimensionless. The area covered by the stored data is contained within the rectangle whose sides are $x = 3\frac{1}{3}$, $x = 11$; $y = -6\frac{1}{3}$, $y = 14\frac{2}{3}$; the grid length is $\Delta x = \Delta y = \frac{1}{3}$. This gives an array consisting of 24 x 26 point values of H at each hour. Since, on the stereographic projection, the mesh is square, it is convenient to carry out all necessary calculations using the Cartesian co-ordinates (x, y) rather than (χ, φ). The following expressions and operators, readily derived from Equations (19) are required in the analysis :

$$\sin\varphi = (1-\alpha^2)/(1+\alpha^2), \quad \cos\varphi = 2\alpha/(1+\alpha^2),$$
$$\frac{\partial}{\partial\varphi} = -\frac{(1+\alpha^2)}{2\alpha}\left\{x\frac{\partial}{\partial x} + y\frac{\partial}{\partial y}\right\}, \qquad (20)$$
$$\frac{1}{\cos\varphi}\frac{\partial}{\partial\chi} = \frac{(1+\alpha^2)}{2\alpha}\left\{-y\frac{\partial}{\partial x} + x\frac{\partial}{\partial y}\right\},$$

where $\alpha^2 = a^2(x^2+y^2)/4R^2$.

The atmospheric pressure p_a on the sea surface is obtained by applying the hydrostatic law so that

$$p_a = 1000 \text{ mb} + \rho_a g H \qquad (21)$$

where ρ_a is the density of air assumed uniform and constant in the vertical between the sea surface and the 1000 mb pressure surface. Then, using (20), the east and north gradients of atmospheric pressure become

$$P = \frac{1}{R\cos\varphi}\frac{\partial}{\partial x}P_a = \frac{\rho_a g(1+\alpha^2)}{2\alpha R}\left\{-y\frac{\partial H}{\partial x} + x\frac{\partial H}{\partial y}\right\},$$

$$Q = \frac{1}{R}\frac{\partial}{\partial\varphi}P_a = -\frac{\rho_a g(1+\alpha^2)}{2\alpha R}\left\{x\frac{\partial H}{\partial x} + y\frac{\partial H}{\partial y}\right\}, \tag{22}$$

respectively. Further the components $(\hat{\omega}_x, \hat{\omega}_\varphi)$ of the geostrophic wind at the surface are given by

$$-2\omega\sin\varphi\,\hat{\omega}_\varphi = -\frac{1}{\rho_a R\cos\varphi}\frac{\partial}{\partial x}P_a,$$

$$2\omega\sin\varphi\,\hat{\omega}_x = -\frac{1}{\rho_a R}\frac{\partial}{\partial\varphi}P_a, \tag{23}$$

so that

$$\hat{\omega}_x = -\frac{1}{2\omega\rho_a}\left\{(1+\alpha^2)/(1-\alpha^2)\right\}Q,$$

$$\hat{\omega}_\varphi = \frac{1}{2\omega\rho_a}\left\{(1+\alpha^2)/(1-\alpha^2)\right\}P \tag{24}$$

Replacing derivatives in Equations (22) by centred differences, so that for example

$$\left(\frac{\partial H}{\partial x}\right)_{x,y} \doteq \left\{H(x+\Delta x, y) - H(x-\Delta x, y)\right\}/2\Delta x$$

and using Equations (24), numerical estimates of $P, Q, \hat{\omega}_x$ and $\hat{\omega}_\varphi$ are obtained at grid points of the 10-level model within the rectangle defined above.

The calculation of surface wind from geostrophic wind requires the use of an empirical law. However, although the optimum formulation of this law has been the objective of investigators for many years, no generally accepted formula has evolved. On the basis of measurements taken in the German Bight, Hasse and Wagner (1971) found that

$$\omega = 0.56\,\hat{\omega} + b, \tag{25}$$

where ω and $\hat{\omega}$ are the magnitudes of surface and geostrophic winds respectively, and b is a constant in the range 1.5ms^{-1} to 3.0ms^{-1} depending upon air-sea temperature differences. For the present work, (25) has been used with $b = 2.4\text{ms}^{-1}$; the value appropriate

to the case of a neutrally stable air column. Two factors influenced this decision. First, the geostrophic wind referred to by Hasse and Wagner is a mesoscale variable calculated from observations of atmospheric pressure at the surface in an area of order 200 km x 200 km. Since the geostrophic wind calculated using (24) involves differences of grid point values of atmospheric pressure over distances $2\Delta x$ corresponding to ~ 200 km, the scales concerned are comparable. Therefore, Equation (25) would appear to be more appropriate here than some of the alternatives, such as the relationships obtained by Findlater, Harrower, Howkins and Wright (1966) between surface wind and observed 900 mb wind, since the latter is a local variable. Second, although the ratio $\omega / \hat{\omega}$ depends significantly on latitude (Hasse and Wagner 1971), Equation (25) can be considered reasonably representative of the region of present interest, since it was obtained from measurements taken within the North Sea. The directions of surface and geostrophic winds are assumed to be the same.

The wind stress on the sea surface is calculated using a quadratic law, so that in components

$$F^{(s)} = c\rho_a \omega_x \sqrt{\omega_x^2 + \omega_\varphi^2} \quad , \quad G^{(s)} = c\rho_a \omega_\varphi \sqrt{\omega_x^2 + \omega_\varphi^2} \quad , \qquad (26)$$

where c is the drag coefficient. Following Heaps (1965) it is assumed that c, depending on wind speed, is given by

$$c \times 10^3 = \begin{cases} 0.565 & \text{for} \quad \omega \leq 5 \\ -0.12 + 0.137\,\omega & \text{for} \quad 5 < \omega \leq 19.22 \\ 2.513 & \text{for} \quad \omega > 19.22 \end{cases}$$

where ω, the wind speed, is in metres per second.

The formulae presented above provide estimates of ρ_a, P, Q, $F^{(s)}$ and $G^{(s)}$ at grid points of the meteorological model, while the input data needed for the surge calculation comprises values at appropriate points of the sea model mesh. These are obtained by interpolation using an extension of the method of differences to two dimensions (Buckingham 1957). The interpolation is carried out on the stereographic plane giving P and $F^{(s)}$ at each point (x', y') say, corresponding to a u-point (x', φ') ; Q and $G^{(s)}$ at each point corresponding to a v-point; and ρ_a at points corresponding to elevation points on the open boundary. The surge input elevation $\hat{\zeta}$ is estimated by applying the

hydrostatic law to the sea and assuming some mean atmospheric pressure, $\bar{p}_a$. Thus

$$\hat{\zeta} = (\bar{p}_a - p_a)/\rho g \,, \qquad (27)$$

with $\bar{p}_a$ taking the value 1012 mb. The computer program written to perform the calculations described produces output which is stored directly on magnetic disc for input to the sea model program.

(c) Application of the data to the sea model

In the preceding section, the treatment of each array of geopotential heights, H , to produce fields of atmospheric pressure gradient, wind stress components and input elevations at one time was described. We now consider the method of applying the processed data through time in the sea model to obtain the surge prediction. Since the meteorological data is grouped in blocks of 13 arrays covering 12 hours taken from each 36 hour weather forecast, it is sufficient to consider a typical 12 hour block.

Suppose the first array of data in such a block consists of values for time $t = t_0$ in the sea model, so that the nth data set corresponds to time $t = t_0 + (n-1)$ hours, and $n = 1,2,3.....,13$. Then the fields of pressure gradients and wind stresses from these data sets are used to calculate ζ, u, v in the sea model in the invervals

$t_0 + \tau \leq t \leq t_0 + n - 1/2 - \tau$ for $n = 1$

$t_0 + n - 3/2 \leq t \leq t_0 + n - \frac{1}{2} - \tau$ for $n = 2,3,\ldots,12$

$t_0 + n - 3/2 \leq t \leq t_0 + 12$ for $n = 13$

where all times are in hours. In order to avoid sudden changes in sea level around the shelf edge, linear interpolation in time was applied to the elevation input $\hat{\zeta}$ within the sea model program.

The preliminary forecasting procedure which results may be summarised as follows :

(i) The collection of observational information and preparation of initial atmospheric fields for 0000 hours is completed by about 0500 hours, when the weather forecast run begins. The run, which requires ~ 14 minutes on the IBM 360/195 computer at the U.K. Meteorological Office, Bracknell, provides data for a 36 hour period starting at 0000 hours, of which hours 6 to 18 are extracted for the present purpose.

(ii) The data is processed to give input data for the sea model covering the interval 0600-1800 hours. The data is stored on magnetic disc. This step takes ~ 2 minutes on an IBM 360/65 computer.

(iii) The storm surge is calculated by the sea model program using the data stored in step (ii) This calculation takes ~ 2 minutes on an IBM 360/65 computer.

Assuming no delays in obtaining access to the computers, the procedure may be completed by 0530 hours, say, and the surge forecast for 0600-1800 hours available at that time. Clearly, the length of warning depends on the section of the weather forecast used and could be increased by taking data for a later 12 hour period. At least 18 hours warning could be obtained by using hours 24 to 36 of each weather forecast instead of hours 6 to 18, though at the expense of some loss in accuracy of the meteorological fields and hence of the surge prediction.

4. COMPUTATION OF SURGES AND DISCUSSION OF RESULTS

(a) Calculations carried out.

From the description of the sea model presented in Section 2 we distinguish four separate versions as follows :

Scheme A : The quadratic law of bottom stress (5) is used with the non-linear equations (1) - (3); on the open boundary radiation condition (11) is applied. This is taken as the basic version of the model.

Scheme B : The same system of equations as in Scheme A is used; radiation condition (13) replaces (11) on the open boundary.

Scheme C : Again the non-linear equations are adopted;

surge elevation is specified on the open boundary using condition (9).

Scheme D : The linear equivalent of Scheme A. The basic equations (1) - (3) are linearised by assuming $D = h$ and taking the linear law of bottom stress (6). Radiation condition (11) is applied on the open boundary.

Surge computations have been carried out using all four versions of the model. In addition to comparing calculated surge elevations and residuals derived from observations, it is of interest to examine differences between solutions obtained using Schemes A, B, and C, which are due entirely to the choice of open boundary condition, and between solutions obtained using Schemes A and D, which are respectively non-linear and linear.

Two surge cases have been considered. For the first period, 26-30 March 1972, solutions were obtained using all of the schemes outlined above. Scheme A was used for the second surge case, 28 March - 6 April 1973. The meteorological situation was very complex towards the end of this period, providing a severe test of the whole forecasting system. Some of the results obtained are now examined in relation to the meteorological situations and compared with observed residuals.

(b) 26-30 March 1972

The meteorological conditions which produced the surge are shown in Figure 3. During the period 26-28 March a large though not very deep depression moved steadily south-eastwards from Iceland, crossing southern Scandinavia before turning north-east into the Baltic and filling slowly. A weak ridge of high pressure reached the North Sea in the early hours of 30 March. The surge residuals derived from observations, plotted in Figure 4, and the co-disturbance lines obtained from Scheme A, shown in Figure 5, indicate that the strong westerly and northwesterly winds acting over the North Sea raised water levels on the Dutch coast and in the German Bight by up to 120 cm.. The changes in elevation occurred slowly producing a very broad surge peak, see Figure 4. Little disturbance was felt on the English coast.

Figure 4 shows that the computations using Scheme A successfully reproduce the surge observed at almost all the coastal stations. Only at Esbjerg, where the computed surge is consistently

30 to 40 cm lower than observed, can the results be considered less than satisfactory. Here the calculated surge values used in the comparison refer to an elevation point some 50 km west of Esbjerg itself, and, since the greatest sea surface slope occurs in the east-west direction, see Figure 5, it seems probable that the deficiency may be substantially accounted for by this fact alone. Surge disturbances introduced on the open boundary following the start of the calculation at 1800h on 26 March from an initial state of rest produce the external surge which can be seen in Figure 4 to propagate from Stornoway to Wick and thence down the east coast of Scotland and England. The erroneous surge peak occurring at Immingham at 0600h on 27 March can be attributed to this cause (see Figure 5). It seems advisable, therefore, to allow a running-in period of at least 24 hours following the start of a computation from zero initial conditions. Thereafter, comparisons between calculated and observed surges can reasonably be made. With this in view, the discrepancies between calculated and observed surges at each port have been quantified by computing root-mean-square (RMS) errors based on hourly values of the difference between the respective elevations for the last three days; 1800h 27 March to 1800h 30 March. For the present solution, the RMS errors thus obtained are typically between 10 and 20 cm; though larger errors appear at Cuxhaven, 23.2 cm, and at Esbjerg, 33.3 cm, and smaller errors at Lowestoft, 9.3 cm, and at Bergen, 7.3 cm..

The solutions computed using Schemes A, B and C, which employ alternative open boundary conditions, are generally similar in the interior of the North Sea and the RMS errors obtained differ by only 2 or 3 cm. However, the differences become more marked at northerly ports as might be expected from their proximity to the open boundary. At Bergen, for example, the RMS error from solution B is almost twice that from solution A, while at Stornoway, a corresponding increase of about 50% is observed. It can be concluded, therefore, that in the present case radiation condition (13), used in Scheme B, is less appropriate than condition (11), used in Scheme A.

The differences between RMS errors obtained from solutions A and C are smaller; typically only 2 or 3 cm. However, the solutions differ considerably in character at ports near the open boundary, as can be seen from Figure 6, which shows the

surge at Stornoway computed using Schemes A, B and C. It is evident that solution C contains a great deal more 'noise' in the form of short period oscillations than either A or B. The source of this noise may perhaps be associated with the reflection of disturbances at the open boundary which results from the use of condition (9). The relative absence of short-period variations from solutions A and B would then be due to the radiation of the associated energy outwards, as permitted in conditions (11) and (13), and its subsequent dissipation in the neighbouring ocean. Although the amplitude of the oscillations in C decreases away from the shelf edge, so that in the interior of the North Sea all three solutions appear to be smooth, a radiation condition, and in particular (11) as used in Scheme A, gives better results overall than are obtained by using (9) to specify elevation on the open boundary as in Scheme C.

The differences between solutions obtained using Schemes A and D may be attributed in the main to the choice of the quadratic law of bottom stress in the former and the linear law in the latter version of the sea model. In the case of linear bottom stress, Equation (6), the effect of tidal currents is taken into account in the choice of the parameter **k** (Weenink 1958). For the quadratic law, the situation is less straightforward. Here the tidal streams influence the total current magnitude, which appears as the term $(u^2+v^2)^{1/2}$ in Equation (5). The effect of tidal friction, which in this case is most conveniently included by computing tide and surge together within the model (Duun-Christensen 1971), is therefore excluded from solution A. Figure 7 shows, as an example, a comparison between the surges at Cuxhaven calculated using Schemes A and D. As would be expected from the above discussion, the linear solution, D, is more strongly damped; the overall surge maximum and the amplitude of variations of shorter duration being reduced as compared with solution A. The difference is reflected in a RMS error at Cuxhaven of 16.3 cm from solution D: about 7 cm less than the corresponding error from solution A. However, such an improvement is not achieved everywhere, and indeed at some locations solution A is more accurate than solution D. Overall, there seems to be little advantage to be gained from taking account of tidal friction by means of the linear law. In fact, the influence of the tide on a storm surge is not simply to increase the degree of

damping, but rather to produce an interaction which is associated with the non-linear terms - including quadratic bottom friction - in the hydrodynamical equations (Proudman 1955 a,b). Tide-surge interaction is of considerable importance in the southern North Sea (Banks 1974), producing oscillations of tidal period in the surge residuals. The semi-diurnal oscillations appearing in the observed residuals at Esbjerg, Cuxhaven and Southend, for example, shown in Figure 4, are probably associated with interaction. The amplitude of the oscillations suggests that the failure of the present solutions to take account of interaction may contribute significantly to the resulting errors. Some priority should be given in the future to modification of the system to allow tide and surge to be computed together within the sea model, thereby taking account of these effects.

(c) 28 March - 6 April 1973

The principal surge activity was confined to the period 1 - 6 April. Meteorological conditions which produced the disturbances are shown in Figure 8. A depression developed west of Ireland in the early hours of 1 April and moved quickly east across northern England, deepening considerably, and entering the North Sea near the Wash at about 1000h on 2 April. Strong northerly winds followed the depression; a wind speed of 65 knots was recorded at Kilnsea at the mouth of the Humber at midday. The depression continued to move east across the German Bight and into the southern Baltic being replaced by a ridge of high pressure extending north-eastwards into the North Sea. A second depression from the Atlantic deepened and moved rapidly north east reaching the Faroes at about 0600h on 4 April. The associated frontal system, bringing with it locally strong southerly and southwesterly winds, crossed the North Sea during the day, leaving a westerly airstream over most areas.

The surge residuals derived from observations at a number of stations are shown in Figure 9, together with the disturbances computed using Scheme A. Co-disturbance lines drawn from the calculated results are shown in Figures 10 and 11, covering the periods 0700h 2 April to 0700h 3 April and 1900h 3 April to 1900h 5 April, respectively. The passage of the first depression into the North Sea near Immingham brought strong westerly winds over the Southern Bight causing levels on the English coast to be

lowered, thus producing the negative surge at Lowestoft, Walton and Southend at 1200h on 2 April. The lowering is reproduced reasonably well by the model, see Figure 9. The discrepancy in magnitude at Southend is probably due to the location of the calculation point some 50 km east of the observation point, this being the direction of greatest surface slope at this time. The strong northerly winds which followed the passage of the depression across the North Sea produced a large positive surge of about 150cm throughout the Southern Bight between 1800h 2 April and 1200h 3 April, see Figures 9 and 10. The splitting of the surge peak at Southend is a well-known effect of tide-surge interaction (Proudman 1955a; Banks 1974). Although the computed result excludes the tidal influence, the timing and height of the surge agree well with observations on the English coast. The approach of the strongest northerlies to the Danish coast caused a negative surge at Esbjerg at 0000h on 3 April, which appears some 3 hours late in the model solution, and a positive surge on the north coast of Holland, which was felt subsequently at Cuxhaven and Esbjerg. The positive surge is badly underestimated by the model, though the reasons for this are not clear. It can only be suggested first, that the meteorological data and its treatment may fail in some instances to give full value to the strongest winds, and second, that the gradients of sea level produced by the winds, which should be greatest in areas of shallow water such as extend along the borders of the German Bight, are undervalued because the sea model fails adequately to represent these areas.

The reduction in levels following the passage of the depression into the Baltic on 3 April is reproduced satisfactorily by the model. Subsequently, however, the most serious discrepancies between the computed and observed levels occur. It is clear from Figure 9 that the large negative surge which affected the east coast of England and the Southern Bight on 4 April is completely absent from the calculated results. Further, the model predicts a positive external surge appearing off the north-west of Scotland at 0700h (Figure 11) and travelling down the east coast to reach Southend at 0000h on 5 April. This surge did not in fact occur. The total effect is to make the computed surge up to 130cm higher than observed for a period of almost 24 hours. The error can be traced as far as Esbjerg early on 5 April. It is not possible to isolate any one circumstance as being responsible

for the large discrepancy here and indeed a number of factors probably acted in combination. All these poor results are associated with disturbances caused by the passage of the frontal system eastwards over the shelf on 4 and 5 April, accompanied by locally strong south or south-westerly winds; the wind direction changing rapidly across the fronts. It is easy to see how the scheme described in Section 3 could introduce errors in such a situation. For example, in taking pressure differences over twice the distance between grid points of the meteorological model (about 200 km), the discontinuity in pressure gradient at a front, perhaps poorly resolved in the first place, could be substantially removed and the resulting geostrophic wind and eventually the wind stress seriously underestimated. Similarly, the deficiencies of the sea model, some of which have already been mentioned and discussed, could compound the error.

For the remainder of the period considered, the agreement between computed and observed surges is satisfactory.

5. CONCLUDING REMARKS

A first system employing numerical finite-difference models of the atmosphere and of the sea to forecast storm surges in the North Sea has been established and applied to two surge cases. The first, a four day period, during which the meteorological situation and consequently surge levels changed slowly, produced good agreement between predictions and observations. For the second period of ten days, with a complex and rapidly changing meteorological situation generating a succession of surges, both positive and negative, in the North Sea, the results were less accurate but nevertheless instructive. Interestingly, the system failed to predict a large negative surge caused by the passage of a frontal system over the Southern Bight.

From the investigations carried out so far, a number of important matters needing further attention can be identified. It seems probable that the present scheme does not adequately represent conditions associated with smaller scale meteorological features such as fronts. Thus, for example, the spatial differencing of values defined at grid points of the meteorological model and the subsequent interpolation to the sea model mesh

introduce smoothing, which tends to remove real discontinuities. The uncertain applicability of the empirical relations between geostrophic and surface wind and of the drag coefficient on the sea surface must also be suspect as sources of error, which could perhaps be removed by combining more closely the models of the atmosphere and of the sea. In addition, the resolution of the present sea model grid does not allow the many areas of shallow water around the Southern Bight and German Bight to be adequately represented, thereby causing further loss of accuracy in the surge predictions. Although some improvement may be possible with the existing mesh size, a model with a considerably finer grid would seem to offer the best long-term answer to this problem. More immediately, the interaction between tide and surge which forms a substantial part of the residual in shallow areas could, with benefit, be taken into account by computing tide and surge together within the present non-linear sea model.

Although a great deal of work remains to be done to improve the accuracy of the results, the potential of the system as a method of storm surge prediction is good. In its present preliminary form, providing 12 hour surge forecasts available up to 18 hours before the start of the period to which they refer, the ability of the scheme to predict the spatial distribution of a surge and its development could make it a useful supplement to existing techniques.

ACKNOWLEDGMENTS

The authors are indebted to Dr. N.S. Heaps for many helpful suggestions and constant encouragement and advice during the execution of this project. The work carried out by members of staff of the Meteorological Office, Bracknell, in particular Mr. R.D. Hunt and Mr. D.E. Jones who provided the meteorological data, and the continued interest and assistance given by Mr. F.H. Bushby and Mr. G.R.R. Benwell is particularly appreciated. Thanks are also due to a number of establishments in Britain and Europe for providing observed water levels or surge residuals.

The assistance of Miss Y. Spruce in preparing the diagrams for publication is gratefully acknowledged.

REFERENCES

BANKS, J.E. 1974. A mathematical model of a river-shallow sea system used to investigate tide, surge and their interaction in the Thames - Southern North Sea region. Philosophical Transactions of the Royal Society, A, 275, 567-609.

BENWELL, G.R.R., GADD, A.J., KEERS, J.F., TIMPSON, M.S. and WHITE, P.W. 1971. The Bushby-Timpson 10 level model on a fine mesh. Scientific Papers of the Meteorological Office, London, 32. 23 pp.

BOWDEN, K.F. 1953. Note on wind drift in a channel in the presence of tidal currents. Proceedings of the Royal Society, A, 219, 426-446.

BOWDEN, K.F. 1956. The flow of water through the Straits of Dover related to wind and differences in sea level. Philosophical Transaction of the Royal Society, A, 248, 517-551.

BRETTSCHNEIDER, G. 1967. Anwendung des Hydrodynamisch-Numerischen Verfahrens zur Ermittlung der M_2 Mitschwingungsgezeit der Nordsee. Mitteilungen des Instituts für Meereskunde der Universitat Hamburg, 7, 65 pp.

BUCKINGHAM, R.A. 1957. Numerical methods. London: Pitman. 605 pp.

DUNN-CHRISTENSEN, J.T. 1971. Investigations on the practical use of a hydrodynamic numeric method for calculation of sea level variations in the North Sea, the Skaggerack and the Kattegat. Deutsche hydrographische Zeitschrift, 24, 210-227.

FINDLATER, J., HARROWER, T.N.S., HOWKINS, G.A. and WRIGHT, H.L. 1966. Surface and 900 mb wind relationships. Scientific Papers of the Meteorological Office, London, 23, 41 pp.

FLATHER, R.A. 1972. Analytical and numerical studies in the theory of tides and storm surges. Ph.D. thesis University of Liverpool.

GROEN, P. and GROVES, G.W. 1962. pp.611-646 in The Sea (ed. M. N. Hill) vol.1. London: Interscience.

HASSE, L. and WAGNER, V. 1971. On the relationship between geostrophic and surface wind at sea. Monthly Weather Review, 99, 255-260.

HEAPS, N.S. 1965. Storm surges on a continental shelf. Philosophical Transactions of the Royal Society, A, 257, 351-383.

HEAPS, N.S. 1969. A two-dimensional numerical sea model. Philosophical Transactions of the Royal Society, A, 265, 93-137.

HEAPS, N.S. 1972. On the numerical solution of the three-dimensional hydrodynamical equations for tides and storm surges. Mémoires de la Société r. des Sciences de Liège, ser.6, 2, 143-180.

LEENDERTSE, J.J. 1967. Aspects of a computational model for long-period water-wave propagation. Rand Corporation Memorandum, RM-5294-PR. 165 pp.

PLATZMAN, G.W. 1958. A numerical computation of the surge of 26 June 1954 on Lake Michigan. Geophysica, 6, 407-438.

PROUDMAN, J. 1953. Dynamical oceanography. London: Methuen. 409 pp.

PROUDMAN, J. 1954. Note on the dynamics of storm surges. Monthly Notices of the Royal Astronomical Society, geophysical supplement, 7, 44-48.

PROUDMAN, J. 1955a. The propagation of tide and surge in an estuary. Proceedings of the Royal Society, A, 231, 8-24.

PROUDMAN, J. 1955b. The effect of friction on a progressive wave of tide and surge in an estuary. Proceedings of the Royal Society, A, 233, 407-418.

REID, R.O. and BODINE, B.R. 1968. Numerical model for storm surges in Galveston Bay. Journal of the Waterways and Harbors Division. Proceedings of the American Society of Civil Engineers, 94, 33-57.

TEMPERTON, C. 1973. Some experiments in dynamic initialization for a simple primitive equation model. Quarterly journal of the Royal Meteorological Society, 99, 303-319.

VELTKAMP, G.W. 1954. De invloed van stationaire windvelden op een zee van op delen constante diepte. Rapport, Afdeeling toegpaste wisbunde Mathematisch centrum, TW24, 37 pp.

WEENINCK, M.P.H. 1958. A theory and method of calculation of wind effects on sea levels in a partly-enclosed sea, with special application to the southern coast of the North Sea. Mededelingen en verhandelingen, K. Nederlandsch meteorologisch instituut, 73, 111 pp.

WILLIAMSON, D. and HASAHARA, A. 1971. Adaptation of meteorological variables forced by updating. Journal of Atmospheric Sciences, 28, 1313-1324.

FIGURES

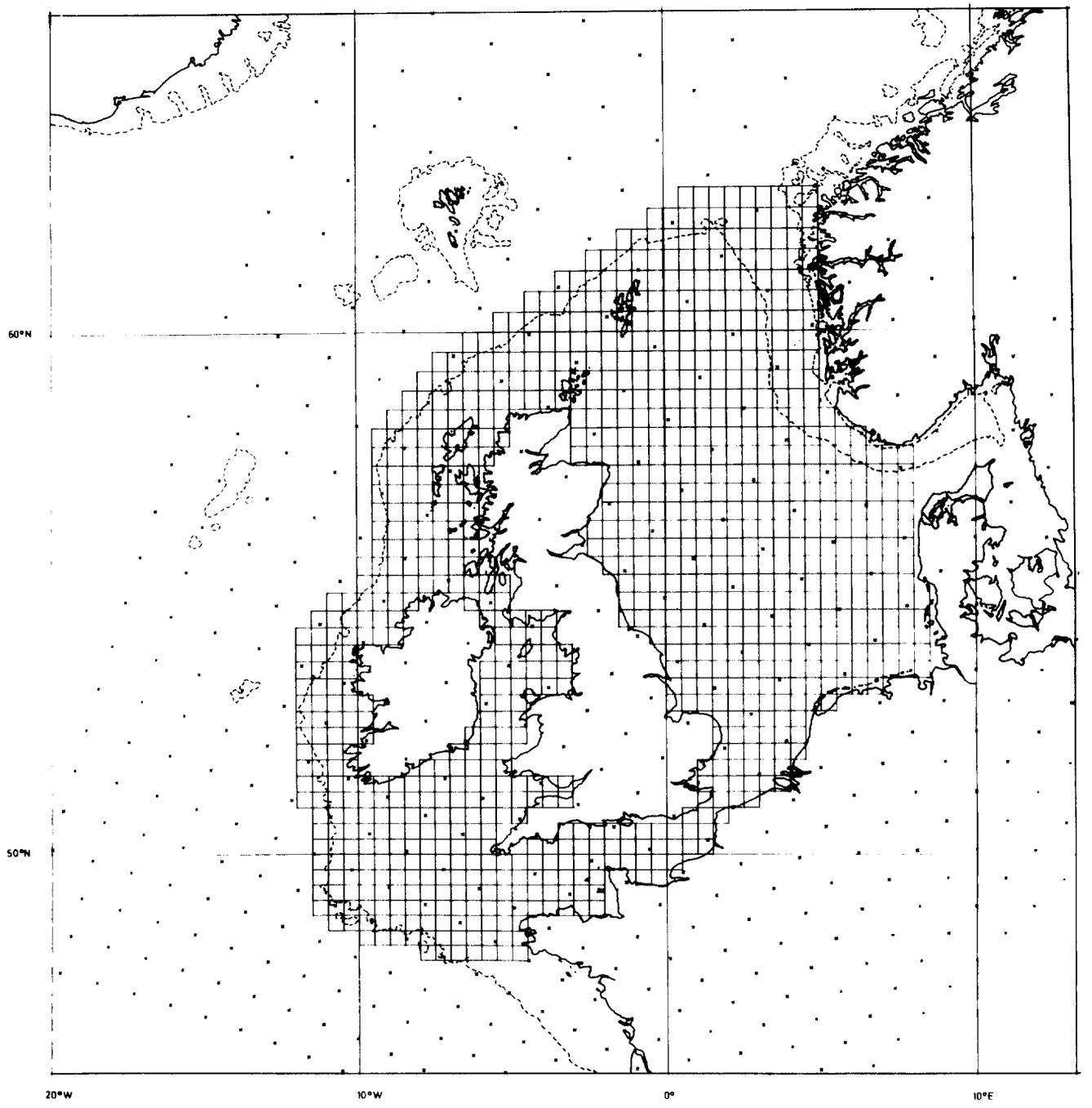

FIG.1: FINITE DIFFERENCE GRID FOR THE NORTH SEA AND CONTINENTAL SHELF USED IN STORM SURGE COMPUTATIONS WITH GRID POINTS OF THE 10-LEVEL METEOROLOGICAL MODEL (X); ----- 100 FATHOM DEPTH CONTOUR.

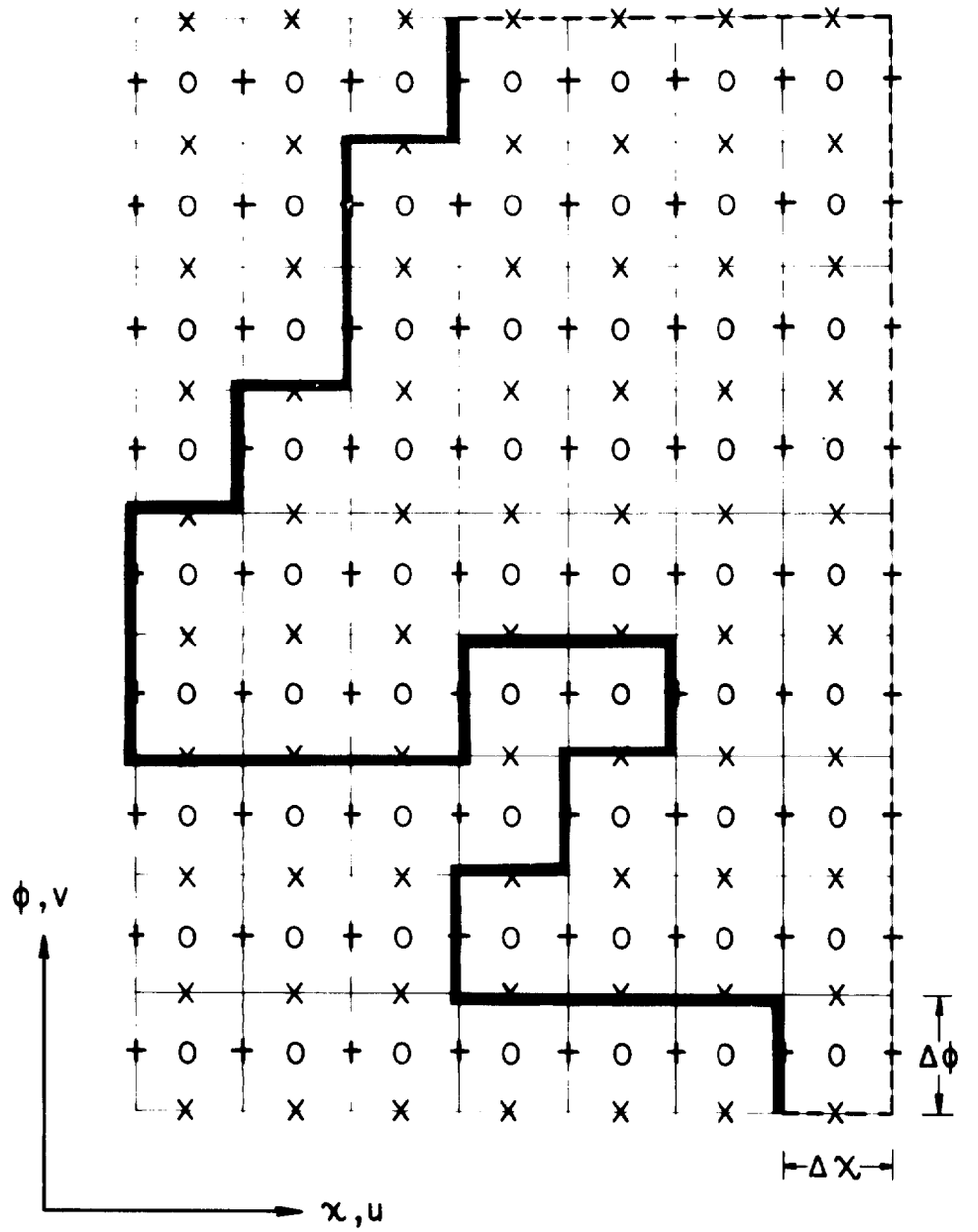

Fig. 2: EXAMPLE OF THE SPATIAL GRID OF THE SEA MODEL.
----- COASTAL BOUNDARY; ——— SEA BOUNDARY;
o, ϛ; +, u; x, v.

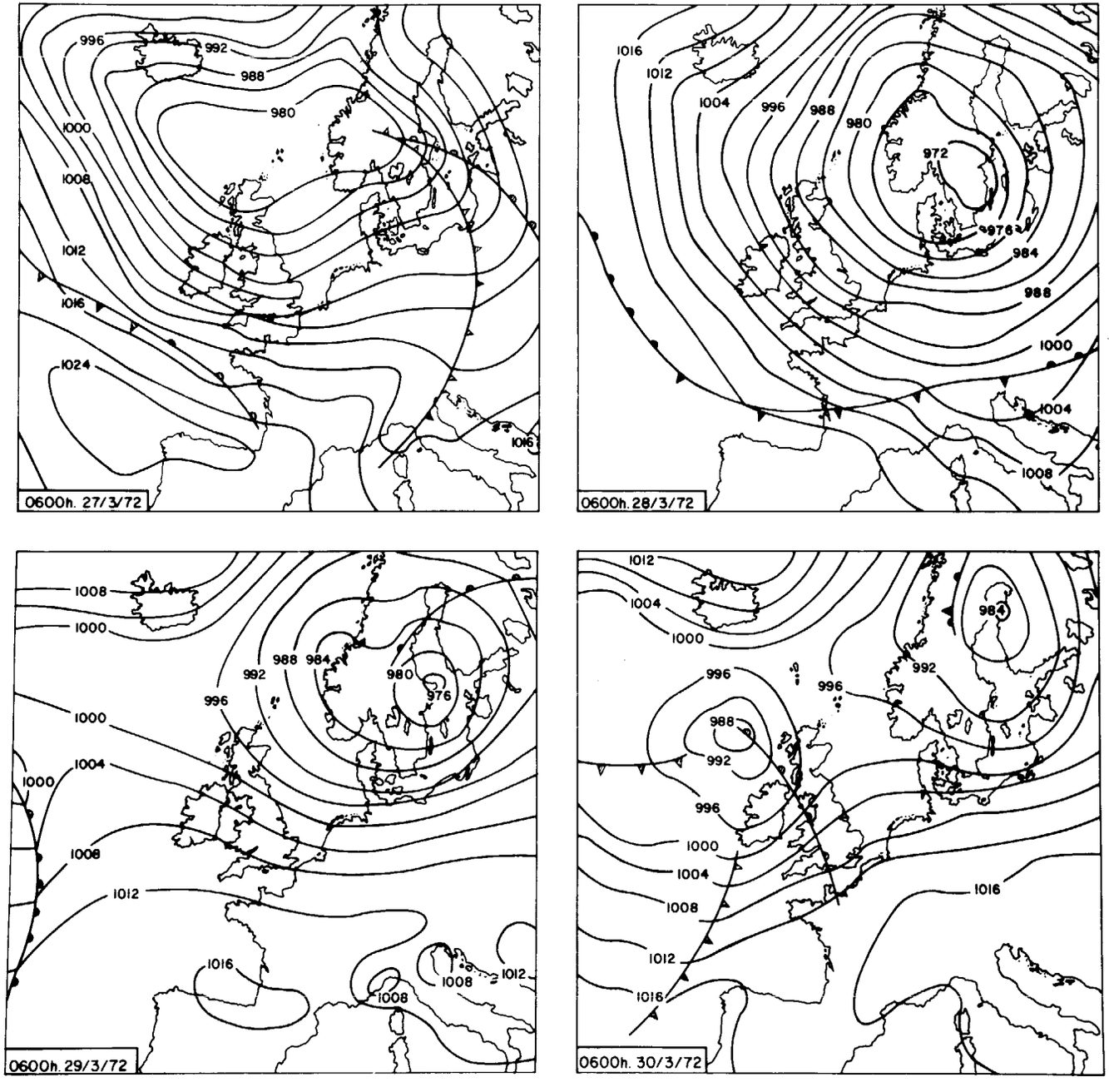

FIG. 3: WEATHER CHARTS FOR THE STORM SURGE OF 26 MARCH TO 30 MARCH 1972.

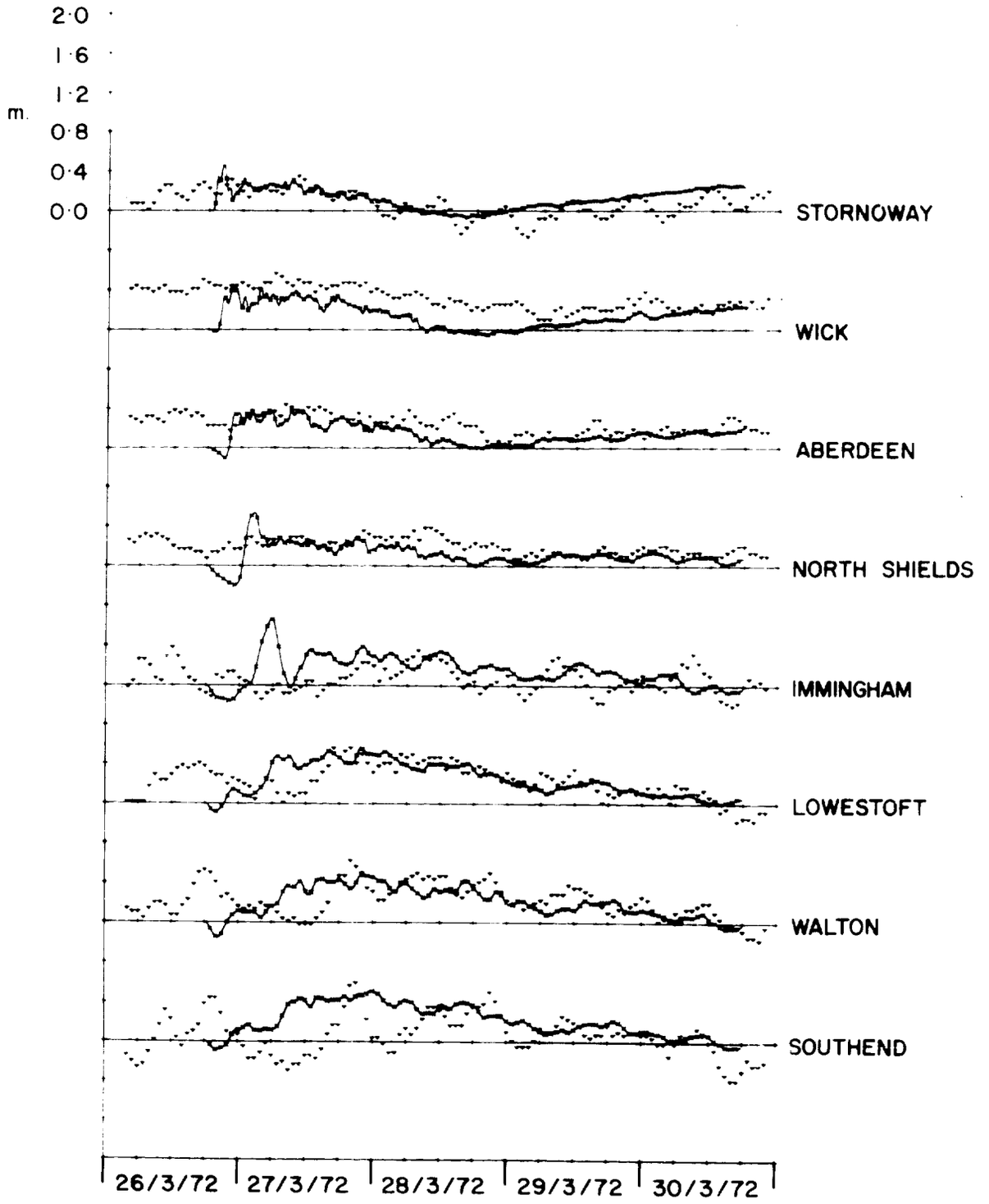

FIG.4a: STORM SURGE OF 26-30 MARCH, 1972 (ENGLISH PORTS).

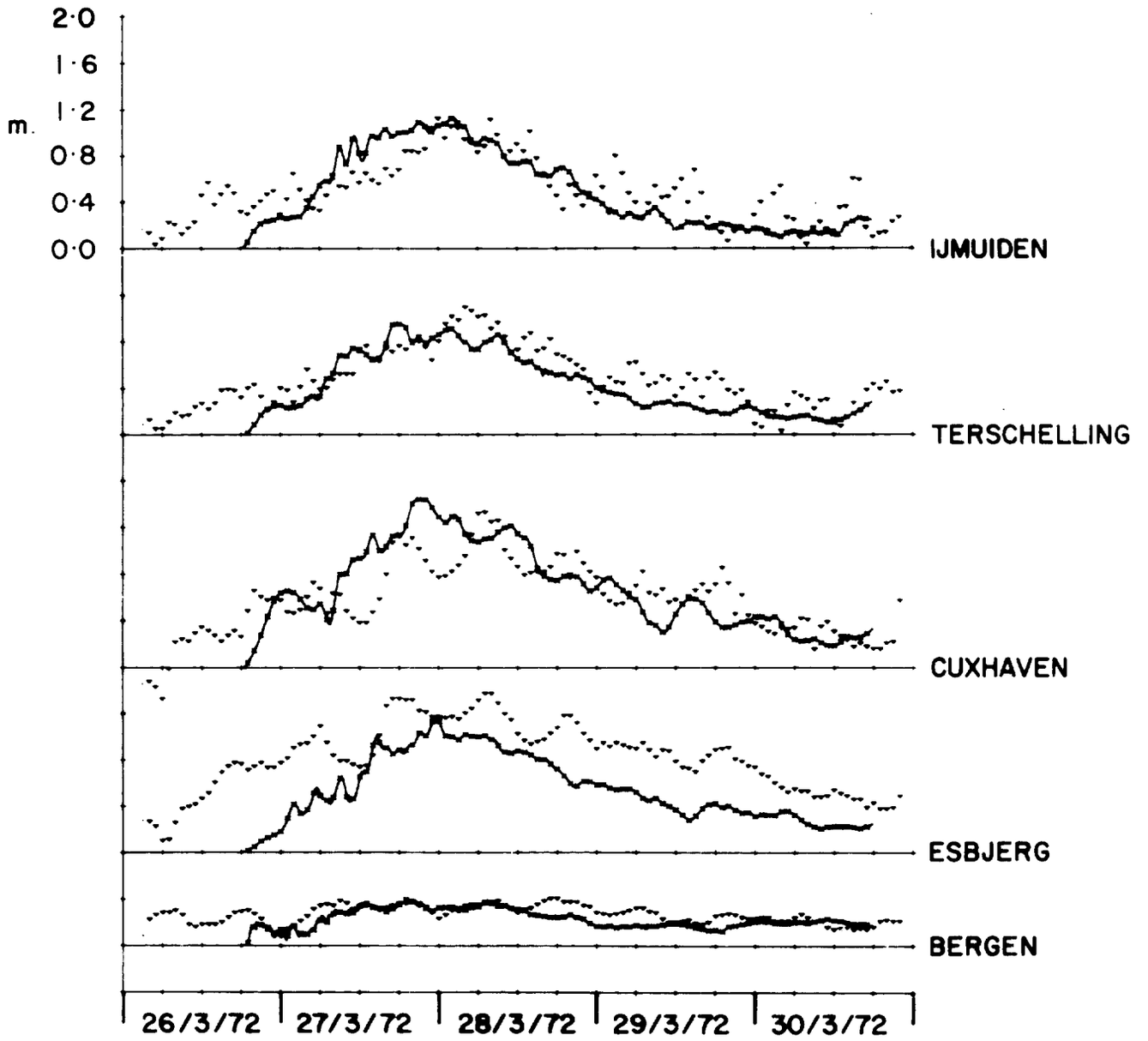

FIG. 4b: STORM SURGE OF 26-30 MARCH, 1972 (CONTINENTAL PORTS).

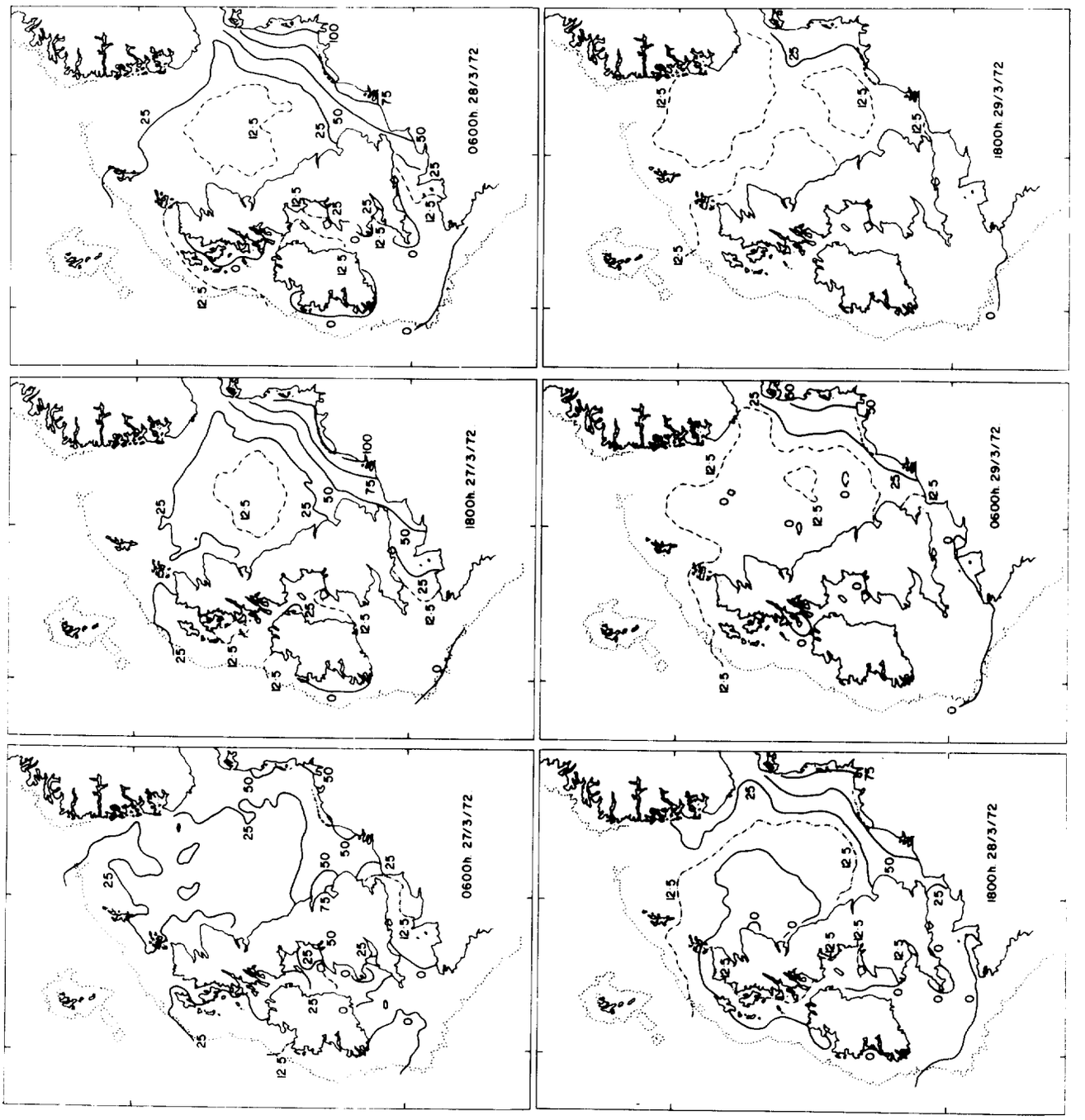

FIG. 5 : CO-DISTURBANCE LINES FOR 26-30 MARCH STORM SURGE.

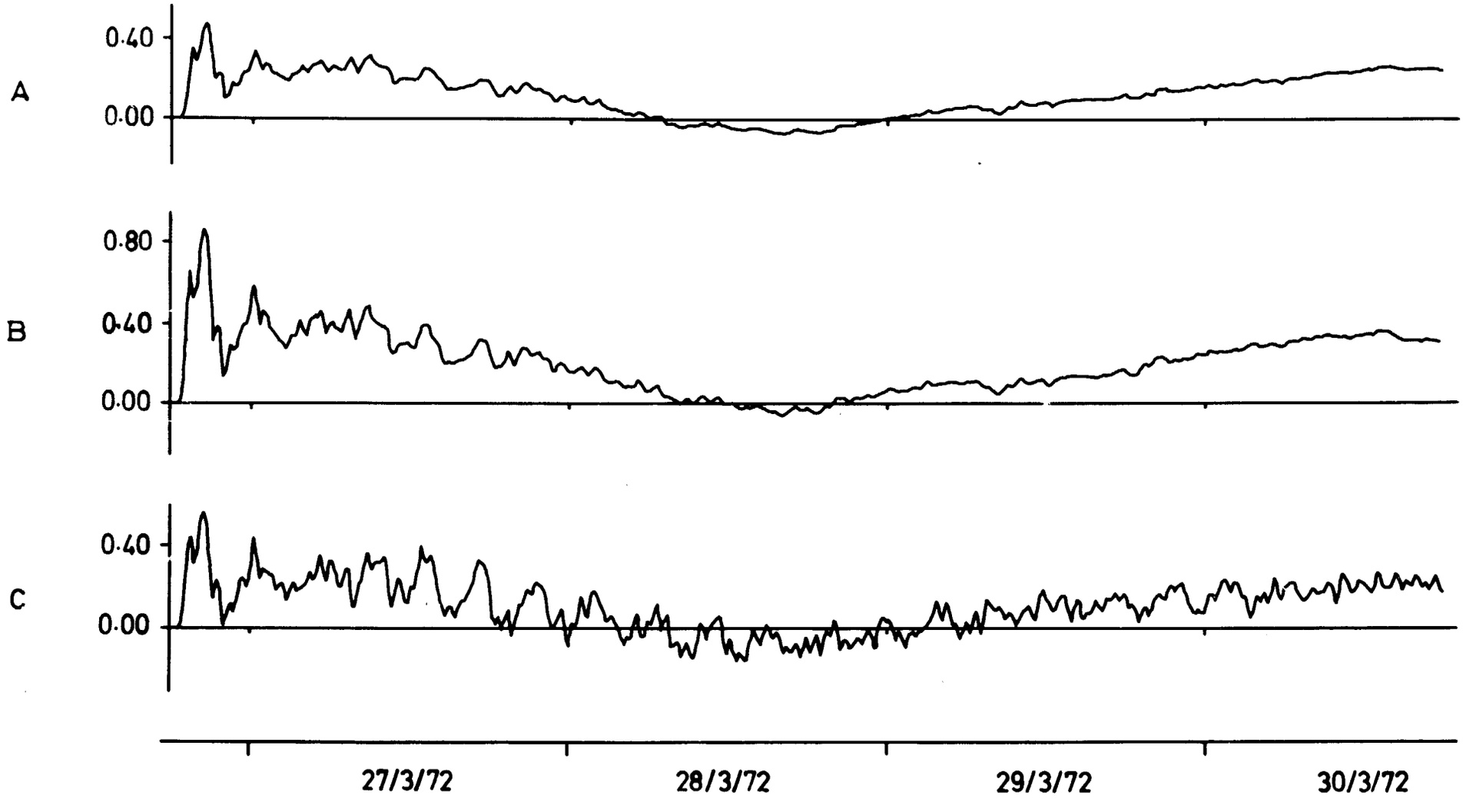

Figure 6: THE INFLUENCE OF DIFFERENT OPEN BOUNDARY CONDITIONS ON THE COMPUTED SURGE AT STORNOWAY.

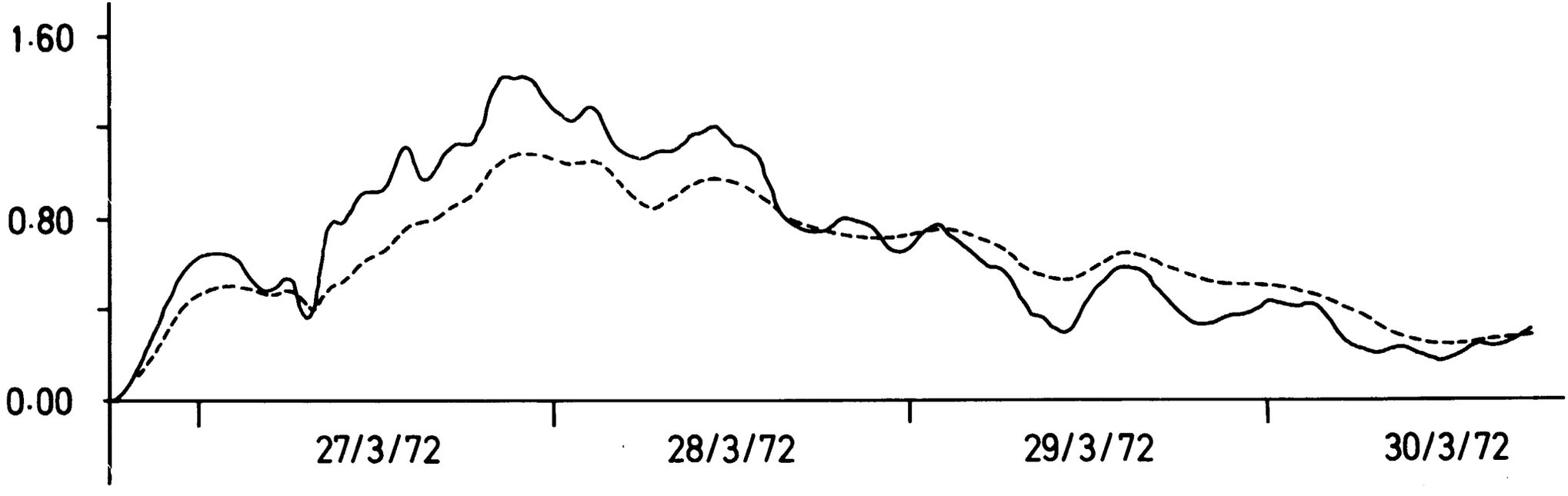

Figure 7: THE SURGE AT CUXHAVEN COMPUTED USING SCHEME A(——) AND SCHEME D(------).

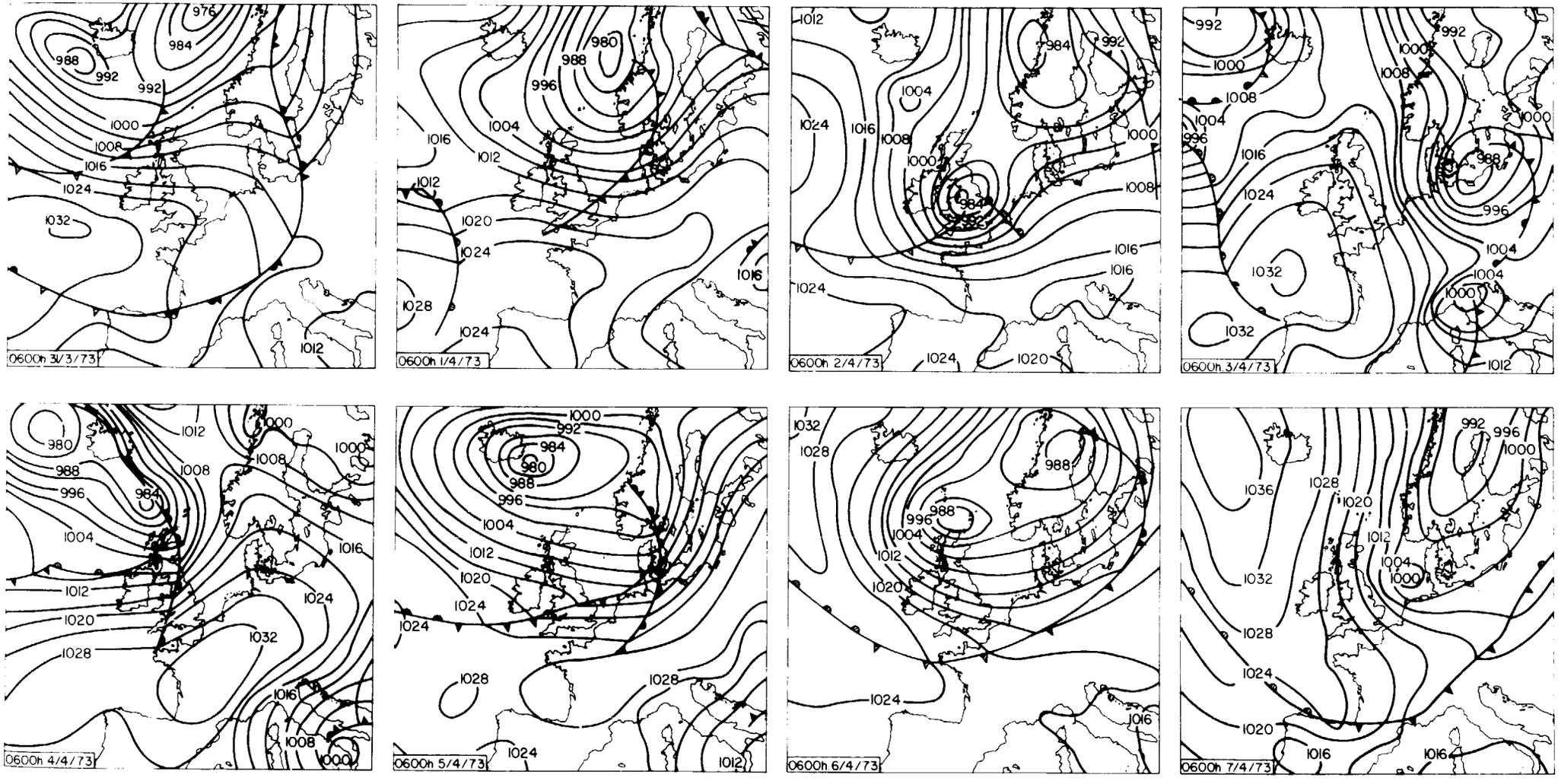

FIGURE 8: WEATHER CHARTS FOR THE STORM SURGE OF 1 TO 6 APRIL 1973

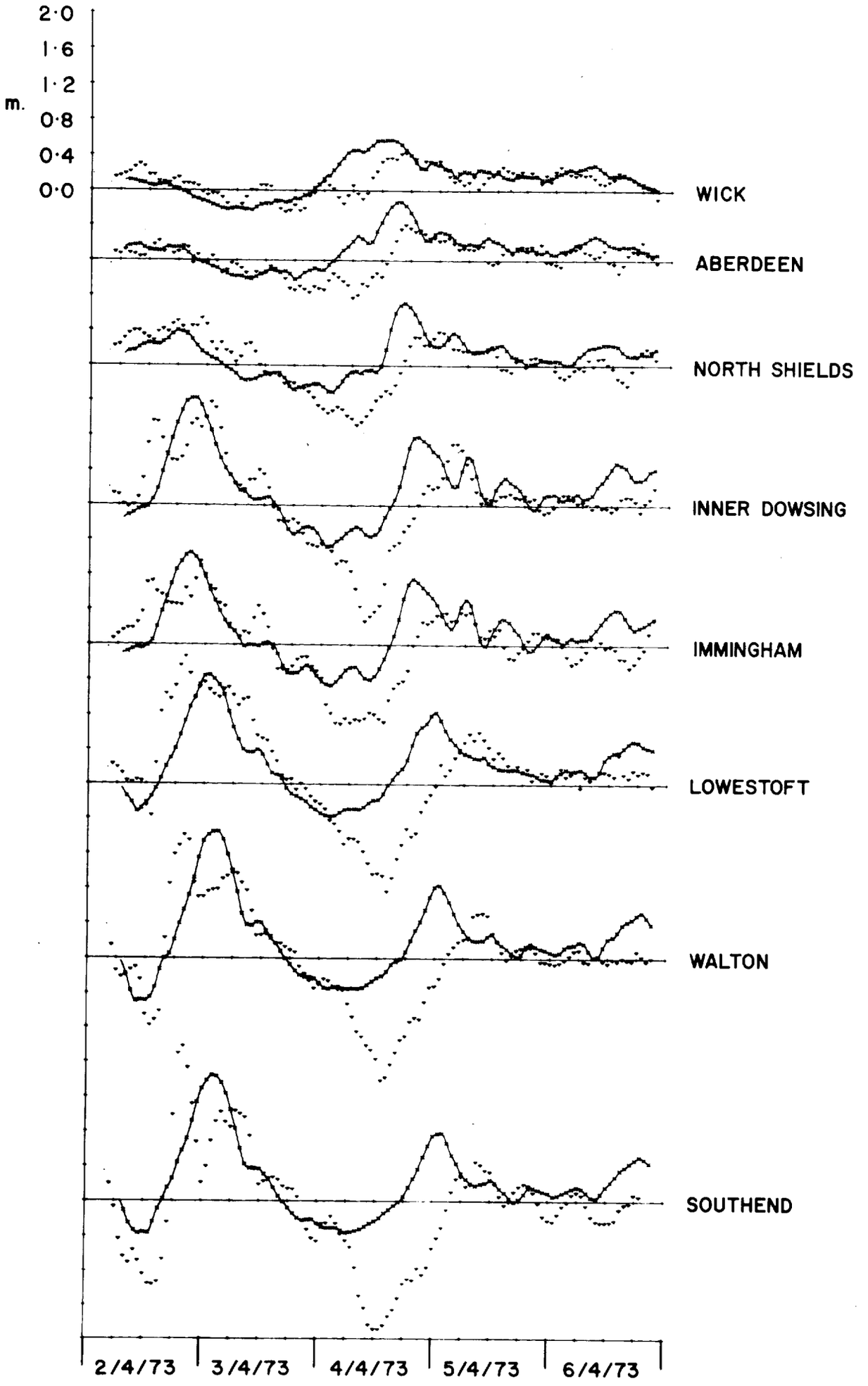

FIG.9a: STORM SURGE OF 1-6 APRIL, 1973 (ENGLISH PORTS).

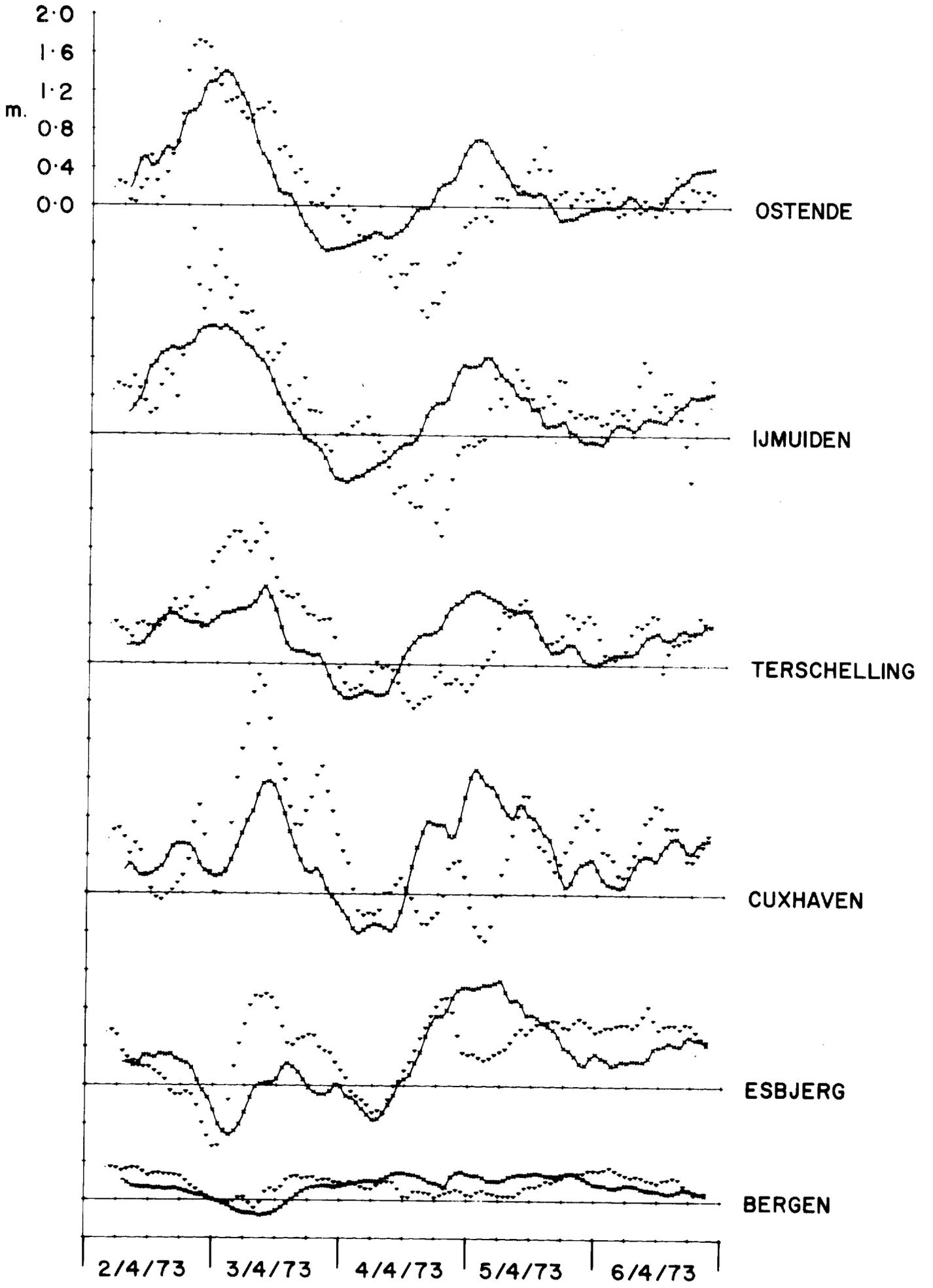

FIG. 9b: STORM SURGE OF 1-6 APRIL, 1973 (CONTINENTAL PORTS).

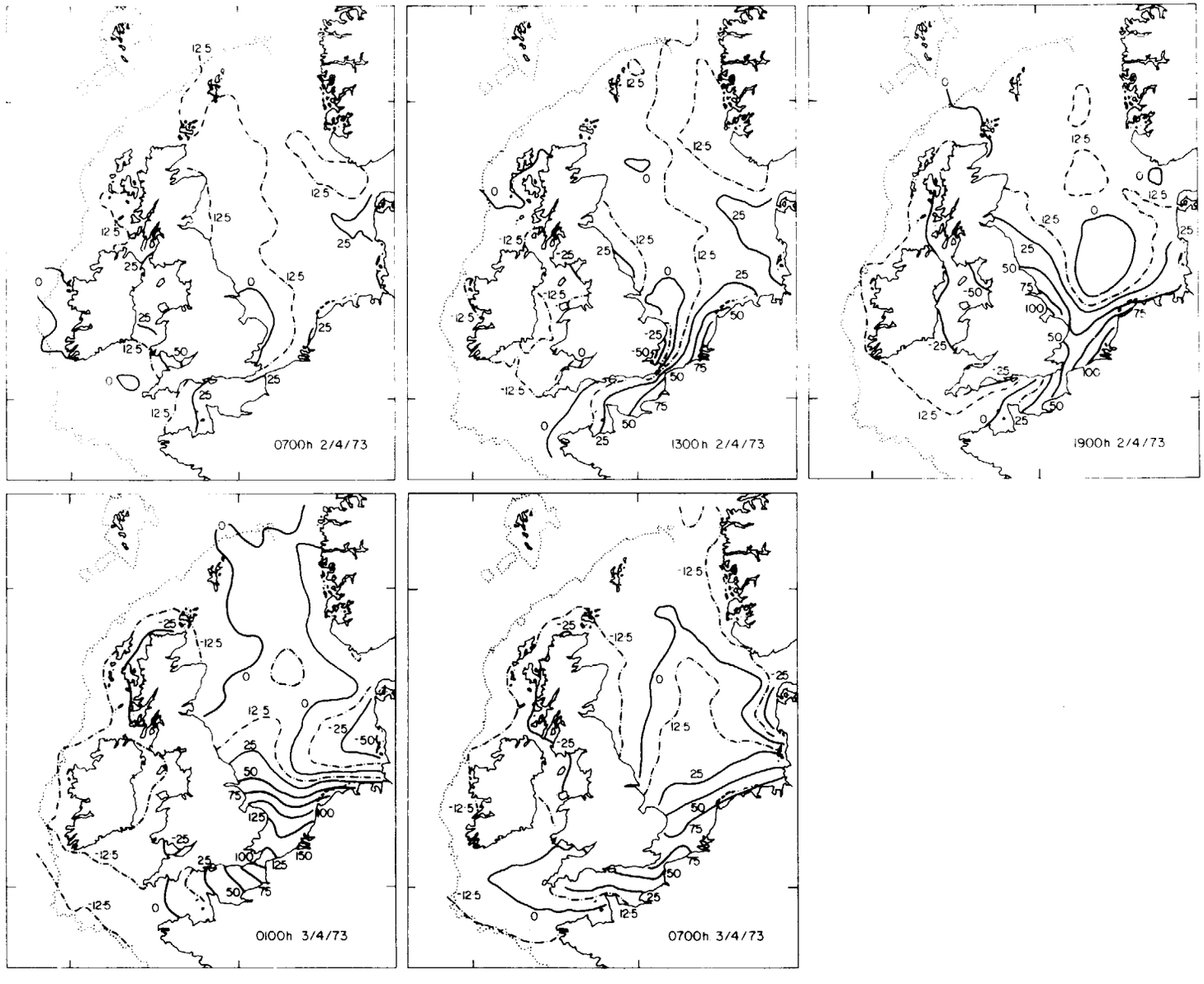

FIGURE 10: CO-DISTURBANCE LINES COVERING THE PERIOD 0700h. 2 APRIL TO 0700h. 3 APRIL, SHOWING ELEVATIONS OF SEA LEVEL IN CM.

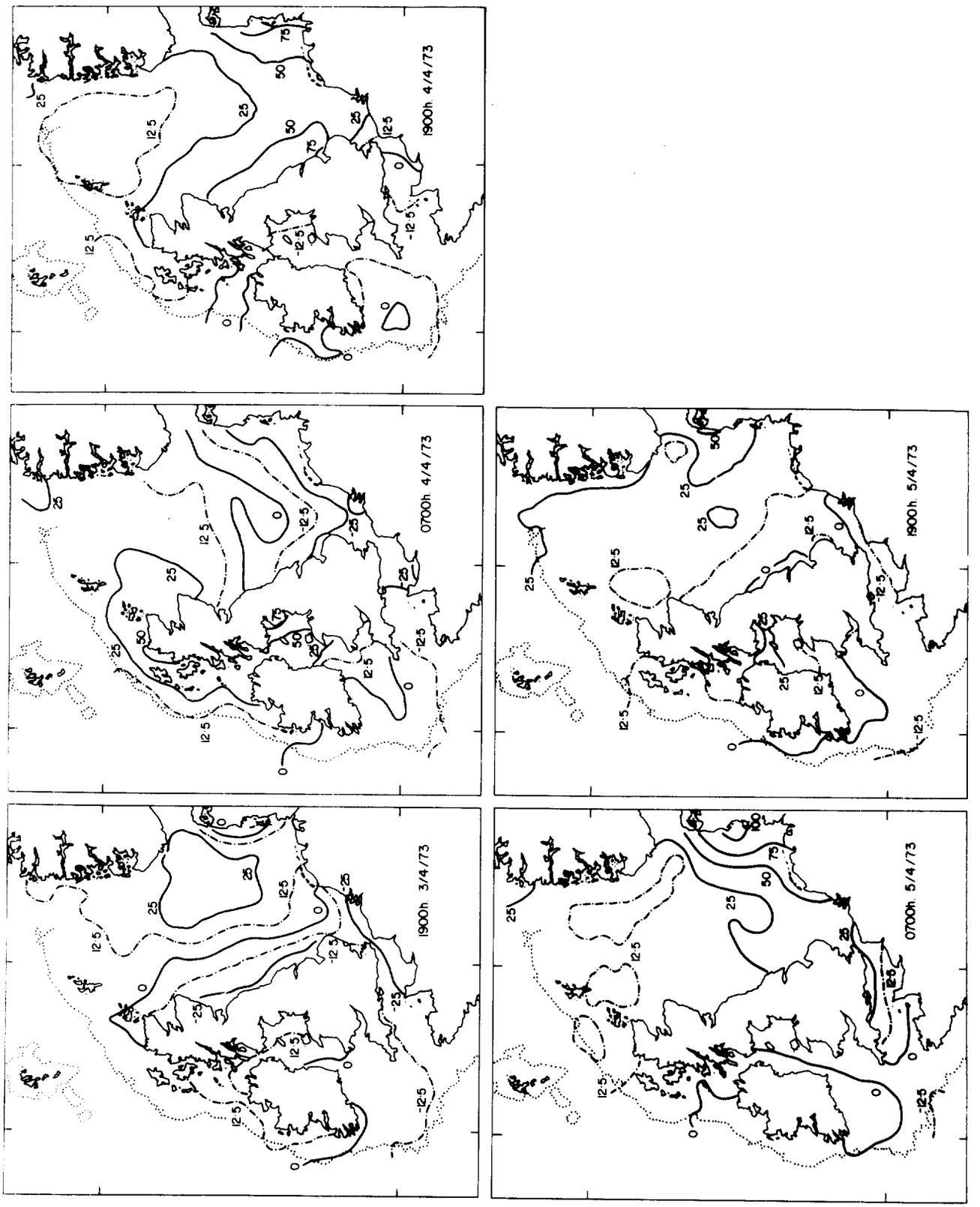

FIG.11: CO-DISTURBANCE LINES FOR 1-6 APRIL STORM SURGE.